Vol. 8, No. 4, 2017
ISSN 2233-4203/ e-ISSN 2093-8950
REVIEW www.msletters.org | Mass Spectrometry Letters

Basics of Ion Mobility Mass Spectrometry

Jong Wha Lee*

Center for Analytical Chemistry, Division of Chemical and Medical Metrology, Korea Research Institute of Standards and Science (KRISS), Yuseong-gu, Daejeon 34113, Republic of Korea

Received November 29, 2017; Accepted December 19, 2017
First published on the web December 31, 2017; DOI: 10.5478/MSL.2017.8.4.79

Abstract : Ion mobility mass spectrometry (IM-MS) combines the advantages of ion mobility spectrometry (IMS) and MS for effective gas-phase ion analysis. Separation of ions based on their mobilities prior to MS can be performed without a great loss in other analytical figures of merit, and the extra dimension of analysis offered by IM can be beneficial for isomer and complex sample analyses. In this review, basic principles of IMS and IM-MS are described in addition to an introduction to various IMS techniques and commercial IM-MS instruments. The nature of collision cross-section (Ω_D), an important parameter determining the transport properties of ions in IMS, is also explained in detail.

Key words: ion mobility spectrometry, ion mobility mass spectrometry, collision cross-section.

1. Introduction

Ion mobility (IM) combined with mass spectrometry (MS) has gained considerable interest from researchers owing to its two-dimensional separation characteristics allowing analysis beyond what is possible with traditional ion mobility spectrometry (IMS) or MS. Although MS is a powerful analytical tool with a broad scope of applications, challenges exist for analyzing complex samples and isobaric analytes. When combined as IM-MS, the IM section offers an additional dimension of analysis to MS, leading to a more informative sample analysis. In return, MS enables clearer identification of the mobility-separated ions based on its high resolution. Due to these reasons, IM-MS has been applied to the analysis of lipids,[1] glycans,[2] metabolites,[3] drugs,[4] polymers,[5-6] and others. IM-MS has also been applied to the fundamental studies of gas-phase ions,[7] and to revealing the structures of biomacromolecules using native MS.[8-11]

Following the growing interests in IM-MS, commercialized IM-MS instruments have become available and contributed to the greater accessibility of the technique.[12-19] However, while MS is familiar to many researchers, the principles of IMS are less well understood due to its major use as a fast on-site screening method.[20] Thus, in this review, basic concepts of IM-MS are introduced with a special attention to the IM technique. Excellent reviews and research papers on IM-MS have previously been published, and the readers are referred to the literature cited herein for more detailed description on individual areas.

IMS can broadly be described as a tool for separating gas-phase ions based on ion mobilities. The term 'ion mobility' is used in the literature to discuss the IMS technique hyphenated to MS (as in 'IM-MS'), but is also a term describing a transport property of an ion denoted as *K*. In the following sections, the unabbreviated term 'ion mobility' is used for describing a property of an ion, and the abbreviation IM is used to discuss the gas-phase separation technique. The combination of IMS and MS is commonly referred to as either 'IMS-MS' or 'IM-MS.' In this review, the latter term is adopted in consideration that ion detection is ultimately carried out at the MS section, and the term 'IMS' is used when the technique is discussed separately from MS.

2. Ion mobility spectrometry (IMS)

2.1 Drift-tube ion mobility spectrometry (DTIMS)

Albeit the recent uses in hyphenation to MS, IMS can be used as a standalone analysis method, which actually was the conventional use for decades.[20-22] In a typical standalone IMS device, ions generated from the source are infused into a drift tube filled with neutral drift gas (also called 'buffer gas'). The ions are accelerated by an electric

*Reprint requests to Jong Wha Lee
E-mail: jongwhalee@kriss.re.kr

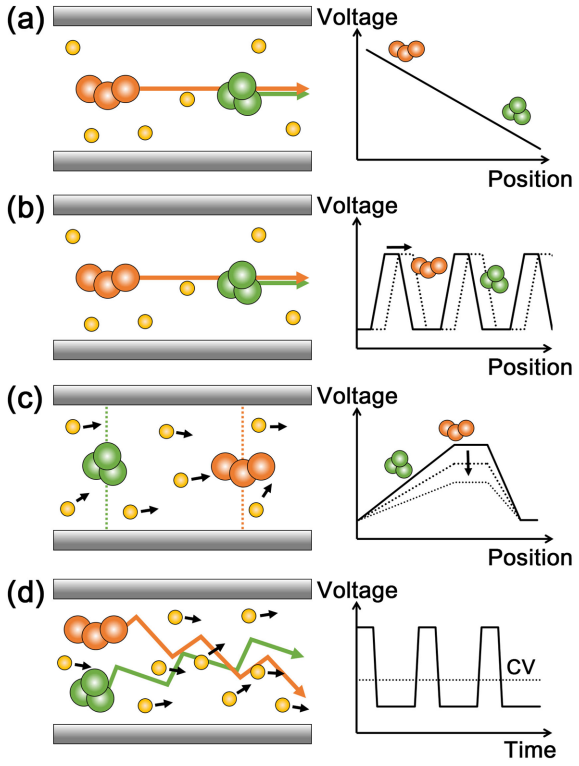

Figure 1. Schematics of various types of ion mobility spectrometry: (a) drift-tube ion mobility spectrometry (DTIMS), (b) traveling-wave ion mobility spectrometry (TWIMS), (c) trapped ion mobility spectrometry (TIMS), and (d) high-field asymmetric waveform ion mobility spectrometry (FAIMS)

field and detected at the exit of the drift tube. The time required for the ions to drift to the exit is recorded, resulting in a chromatogram of ion signal versus drift time (t_d). Despite the large variations between the available IMS techniques, drift-tube IMS (DTIMS) can be regarded as the most basic type. In DTIMS, the electric field is uniform and the drift gas is stationary (Figure 1a). Under such conditions, ions undergo repeated collisions with drift gas molecules and reach a steady state in terms of macroscopic drift velocity (v_d). In a weak electric field, the drift velocity is proportional to the field strength (E).[23-24]

$$v_d = KE = \frac{L}{t_d} \tag{1}$$

The proportionality factor K in eq 1 is a characteristic property of an ion that is referred to as the ion mobility. Because the drift velocity can be evaluated directly from the drift tube length (L) and the measured drift time of the ion (t_d), ion mobilities can be determined from DTIMS experiments. For analytical purposes, measured mobilities of ions can be compared with those listed in a mobility library to identify components in a sample.[25]

Interestingly, the simplicity of the conditions used in DTIMS (two-body collisions, uniform electric field, stationary drift gas, etc.) enables highly accurate theoretical characterization of ion behaviors during the process. For example, the maximum resolving power of a DTIMS instrument limited by thermal diffusion of ions along the transmission axis is predicted as follows:[26]

$$\frac{t_d}{\Delta t_d} = \frac{1}{4}\left(\frac{V_{ez}}{k_B T \ln 2}\right)^{1/2} \tag{2}$$

where Δt_d is the full width at half maximum (FWHM) of a peak in a drift time chromatogram, V is the applied voltage, e is the elementary charge, z is the ion charge state, k_B is the Boltzmann constant, and T is the temperature of the drift gas. The resolving power predicted by eq 2 should be regarded as the maximum possible resolving power, which may be reduced by other factors such as the spread of the ions after injection into the drift tube, space charge, and net gas flow or temperature variation inside the drift tube.[27-28] Still, it is possible to predict if ions with similar mobilities could be separated at all. It also follows from eq 2 that the resolving power of a DTIMS instrument is primarily dependent on the applied voltage, if ion charge state and drift-tube temperature are constant. It is also possible to infer that highly charged ions (i.e. large z) would display sharper peaks.

Another interesting characteristic of DTIMS is that the mobility of an ion measured under a weak electric field is directly related to its orientationally-averaged collision integral, Ω_D:[23-24, 29]

$$\Omega_D = \frac{3ez}{16N}\left(\frac{2\pi}{\mu k_B T}\right)^{1/2}\frac{1}{K} \tag{3}$$

where N is the drift gas number density and μ is the reduced mass between the ion and drift gas. Equation 3 and Ω_D are commonly referred to the Mason-Schamp equation and collision cross-section (abbreviated as CCS), respectively, but it should be noted that a recent publication suggests that the terms 'fundamental low-field ion mobility equation' and 'collision integral', respectively, are more adequate.[30] In any case, ion Ω_D can roughly be described as the effective area of the ion in which collisions with drift gas molecules can occur. However, unless the collision partners are assumed as hard spheres, the concepts of 'area' and 'collisions' are vague in the microscopic world, and whether a 'collision' has occurred is ultimately determined by the change in the molecular trajectory.[31] The change in the molecular trajectory due to a collision can be described using the scattering angle (θ), which is dependent on temperature, initial relative velocity and orientation between the collision partners. Therefore, Ω_D can be written as:[30,32]

$$\Omega_D = \frac{1}{2}(kT)^{-3}\int_0^\infty Q_D \exp\left(-\frac{\varepsilon}{kT}\right)\varepsilon^2 d\varepsilon \tag{4}$$

where ε is the relative collision energy. Q_D is the

momentum-transfer cross section that is defined as follows:

$$Q_D(v_r) = 2\pi \int_0^\infty [1 - \cos\theta(v_r, b)] b db \quad (5)$$

where v_r is the relative velocity and b is the impact parameter. Equations 4 and 5 illustrate that Ω_D is a well-defined property of an ion,[30] and eq 3 shows that this property is related to ion mobility K measured using DTIMS. The good understanding of ion behaviors in DTIMS is advantageous in various aspects including characterization of unknowns and standardization of measurements.[33]

2.2 Characteristics of collision cross-section (Ω_D)

Ω_D of an ion is dependent on its size and shape. Ω_D is typically expressed in units of Å^2 or nm^2 (~100-300 Å^2 for small organic ions, ~500-2000 Å^2 for small, compact polypeptides and proteins, and >3000 Å^2 for protein complexes and particles, for ions in helium and at near room temperature), with the latter unit more common for macromolecular ions. Because ion separation in low-field IMS (the concept of 'low field' is described later) is primarily dependent on ion Ω_D, IMS could be described as a tool for ion structural separation. However, although such description is simple, it is not entirely accurate. As eq 4 shows, Ω_D is a complicated parameter that needs to be explained in detail.

At a first glance, eq 3 contains factors such as z, N, μ and T. Thus, it may appear that Ω_D is a parameter from K that has been corrected for ion charge state, drift gas pressure, drift gas type, and temperature, and that these factors no longer affect Ω_D. However, all of these factors affect Ω_D, and understanding these dependences is important for understanding the nature of Ω_D and the fundamentals of IMS.[34]

2.2.1 Drift gas

Firstly, although the inclusion of μ in eq 3 addresses the change in the momentum-transfer efficiencies during two-body collisions between ions and drift gas, Ω_D is still dependent on the choice of the drift gas (Figure 2a). This is because in a strict sense, Ω_D of an ion is not a measure of a vague quantity such as 'size', but is actually representative of ion-drift gas interaction characteristics. Conceptually, changing the drift gas is similar to changing the stationary phase in chromatography. Therefore, the Ω_D of an ion varies in different drift gases and Ω_D values should be supplied with the information on the drift gas composition in which the measurement was performed.[34] For fundamental studies, helium has been the most common drift gas due to its simplicity enabling accurate theoretical characterization of ion-drift gas interactions. Nonetheless, other drift gases including nitrogen, argon, carbon dioxide, air, gas mixtures, etc. have also been used for various purposes.[12, 34-36] It is possible to achieve improved separation by altering the drift gas,[36] analogous to the possible improvement in peak separation with a change in the stationary or mobile phase in chromatography. As an example, addition of chiral 'dopants' in drift gas can facilitate chiral ion separation using IMS, which is not possible with conventional achiral drift gases.[37]

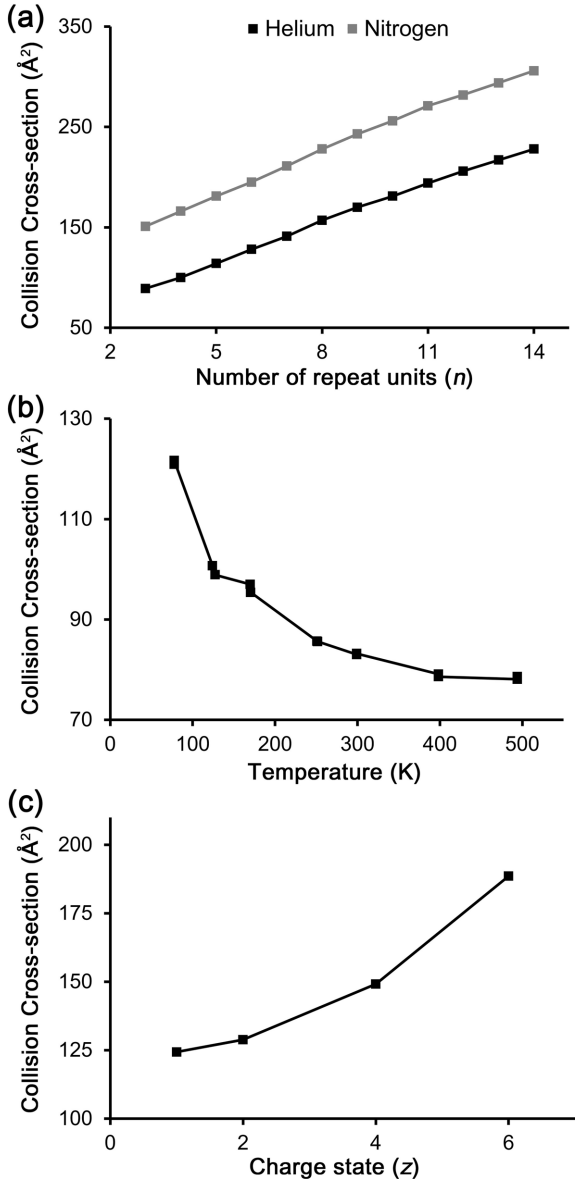

Figure 2. The dependence of ion collision cross-section on (a) drift gas and ion size, (b) temperature, and (c) charge state. The data are for polyalanine (n = 3–14; ref 77), tetraglycine (ref 42), and C_{60} (ref 41) for (a), (b), and (c), respectively. Values in (c) are theoretically predicted values.

2.2.2 Temperature

Temperature-dependence of Ω_D is an interesting phenomenon that is also important for understanding the nature of Ω_D. In the case of flexible ions, Ω_D increases with the increase in temperature, because ions can adopt more elongated structures at high temperatures.[38] On the other hand, for structurally rigid ions, Ω_D generally increases with the *decrease* in temperature (Figure 2b).[39-41] Simply stated, this is because at low temperatures, ions interact more effectively with the drift gas due to the decrease in the kinetic energy of the drift gas.[39,42] The dependence of ion Ω_D on temperature is especially greater in drift gases with high polarizabilities.[41-42] Typically, the variation in Ω_D across a narrow range of temperatures is small (smaller than the imprecision of a Ω_D measurement), and Ω_D measured under ambient temperatures may grossly be expressed as 'Ω_D at room temperature.' However, a large body of IMS experiments in the literature were performed at high temperatures to prevent clustering of water or drift gas molecules on ions of interest.[25,43-44] Such a large difference in temperature is sufficient to cause a significant difference in Ω_D, and it is therefore necessary to note the temperature at which Ω_D measurement was performed.

2.2.3 Charge state and charge distribution

Ions with similar structures but different charge states (z) can have considerably different Ω_D (Figure 2c).[41, 45-47] As was the case for temperature-dependence of Ω_D, this is because ions with greater charge states interact more strongly with the drift gas. More interestingly, even ions with identical total charge, but different charge distributions, can display significantly different Ω_D.[35,45-46,48-49] As are the temperature effects, the charge and charge distribution effects are also greater in drift gases with higher polarizabilities.[35,41,48-49]

2.2.4 Inaccurate measurements

Some factors reduce the accuracy of experimentally measured Ω_D. Though Ω_D itself has a rigorous definition[30] as in eq 3 and should not depend on electric field E and drift gas number density N, *experimentally evaluated* Ω_D is dependent on E and N because the relationship in eq 3 that is used to correlate experimental observables to Ω_D is truly accurate only at a vanishingly small electric field.[23,30,50] Whether a field is weak or strong in IMS is discussed in terms of E/N, because an electric field accelerates the ions while collisions with drift gas molecules decelerate ions (in average), and the frequency of collisions is proportional to N. At high E/N, eq 3 becomes increasingly inaccurate, making experimental Ω_D evaluated under high E/N conditions inaccurate.[50]

Finally, ion mobility measurements are also affected by several factors including inaccurate measurement of temperature and pressure, inhomogeneous electric field, and others.[28] Although many studies have demonstrated exceptional precisions for the measured Ω_D or K, it is not challenging to find two 'precise' experimental values not agreeing within the claimed range of uncertainties. This is partly because the reported precisions represent only the repeatability rather than interlaboratory reproducibility. Furthermore, although measurement bias is not removed by repeated measurements, it is common to estimate measurement uncertainties solely based on measurement repetition. Fortunately, the deviations between Ω_D measured in different laboratories are not large, and the concepts of uncertainty evaluation and measurement standardization are beginning to be adopted in the field.[28, 33, 51-54]

2.3 Collision cross-section (Ω_D) and ion structures

In a given drift gas and temperature, Ω_D generally increases with increasing ion size (Figure 2a). For similarly structured ions, the increase in Ω_D is slower than the increase in ion m/z because m/z is roughly proportional to L^3 (assuming constant density), whereas Ω_D is related to L^2. Exact correlations between Ω_D and m/z differ for ions belonging to different chemical classes,[13] which could enable convenient characterization of unknowns based on previously determined correlations.

It is interesting to note that in case of molecular clusters with identical m/z, multimeric ions typically show smaller drift times than monomeric ions.[55] For example, if a singly protonated ion at m/z 1000 coexist with a doubly protonated, dimeric cluster ion at m/z 1000 ($z = 2$), the two ions are not distinguished by MS. On the contrary, in IMS, the influence of the electric field is doubled with the two-fold increase in z, whereas a two-fold increase in mass typically does not result in a two-fold increase in Ω_D. Therefore, the dimeric ion travels faster than the monomeric ion across the drift tube, allowing discrimination using IMS. It is worthwhile to consider that an increase in ion mass also increases the momentum loss during a collision, causing a reduction in ion mobility. This effect is determined by the reduced mass μ between the ion and drift gas molecule, which, for sufficiently large ion and small drift gas, is not greatly dependent on the change in ion mass.[56-57] Thus, the effect can be neglected in the majority of the conditions. However, it has been shown that in some cases the μ effect can lead to isotopologue separation.[56]

A more accurate characterization of ion structures using IMS is further possible based on theoretical calculations of Ω_D.[7-8,58] This unique capability of IMS stems from the existence of an accurate relation (eq 3) that bridges experimentally measured ion mobilities with a well-defined characteristics of an ion, Ω_D.[23-24,29] Apart from the experimental determination of ion Ω_D using eq 3, a theoretical estimation of the Ω_D of three-dimensional structural models of ions is also possible. Then, the agreement between the experimental and theoretical Ω_D can be examined to probe ion structures. For example, if

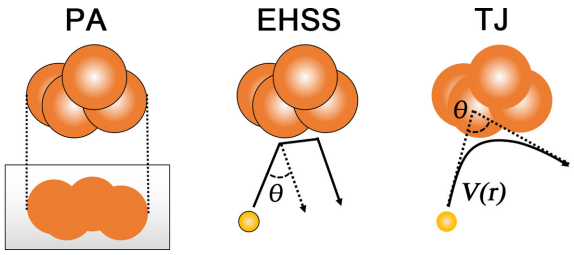

Figure 3. Schematics of the three most common theoretical collision cross-section calculation methods: projection approximation (PA), exact-hard spheres scattering (EHSS), and trajectory (TJ).

one was interested if a protein ion is in a compact or an elongated form in the gas phase, one can compare the experimental Ω_D of the protein ion with the theoretical Ω_D of its compact or elongated structural model.[59]

Various methods are available for theoretical Ω_D calculations, and the most commonly used methods are projection approximation (PA),[47] exact hard-spheres scattering (EHSS),[60] and trajectory (TJ),[40] each adopting different models on ion-drift gas collisions (Figure 3). The PA model approximates Ω_D as the orientational average of projected hard-sphere areas of an ion. Although the concept of projected areas greatly simplifies the description of Ω_D, it is based on an approximation of the definition of Ω_D shown in eq 4. The model is reasonably accurate for small ions with convex structures, but becomes increasingly inaccurate for large ions with concave structures.[60] The EHSS model (Figure 3) explicitly simulates the ion scattering process for more accurate description of ion-buffer gas collisions.[60] However, the model still considers the atoms in ions and drift gas as hard spheres with predefined radii, and subtle characteristics of Ω_D described in the above subsection (temperature or charge-state dependence, etc.) cannot be reproduced. The TJ method (Figure 3) most faithfully follows the definition of Ω_D in eq 4 and performs simulations of drift gas trajectories based on realistic representation of intermolecular interactions ($V(r)$).[40] As the TJ calculations are computationally costly, various other methods have been developed for faster theoretical estimation of Ω_D.[32,61-66] Note that most of the Ω_D calculation methods are aimed at providing Ω_D values in helium due to the simplicity of the drift gas. For Ω_D calculations in nitrogen drift gas, a modified TJ method has been developed,[67-68] and later reparametrized.[35,69]

Despite the successful combination of experiment and theory for ion structural studies, the accuracy of theoretical Ω_D calculations has not been clearly characterized. Therefore, careful interpretation of calculation results is necessary.[69-72] A recent publication and an ongoing study are focused on developing well-characterized theoretical tools for Ω_D calculations,[71,73] which are expected to contribute to higher reliability of IMS-based structural studies.

2.4 Traveling-wave ion mobility spectrometry (TWIMS) and trapped ion mobility spectrometry (TIMS)

Having discussed the core parameter determining ion separation under low fields, different types of IMS are described below. Traveling-wave ion mobility spectrometry (TWIMS) and trapped ion mobility spectrometry (TIMS) are recently developed ion mobility techniques that are almost exclusively used in combination with MS rather than in standalone devices. However, for simplification of the discussions, the techniques are described in this section as if they are being used separately from MS.

In TWIMS, the electric field used is not static nor uniform. The applied electric field is in the form of 'potential waves' traveling across the drift tube (Figure 1b). The traveling wave technology was initially developed for effective transport of ions in stacked ring ion guides (SRIGs).[14] However, it was discovered that the technique can facilitate mobility separation of ions, and was integrated with MS.[14,55,74] Ion separation in TWIMS is achieved by rollover of ions surfing on a wave-front to the next wave-front due to collisional impediment of ion motion by drift gas.[14,75] If ions are too mobile in a drift gas, the ions surf on a single wave-front without rolling over to the next wave-front and mobility separation is not achieved.[76] Thus, to maximize the resolving power, mobilities of ions need to be sufficiently reduced.[76] and high polarizability gas such as nitrogen is typically used for effective mobility separation using TWIMS.[14-15]

An important difference between TWIMS and DTIMS is that ion motion in the former is not completely understood, making it difficult to relate the measured drift times with Ω_D. Therefore, it is difficult to compare the drift times obtained under different TWIMS experimental conditions, such as different pressures and traveling-wave parameters (wave velocity and height). Nevertheless, it is possible to calibrate the drift times from TWIMS experiments to ion Ω_D.[9-10,77-78] The calibration is performed by measuring the drift times of a set of ions whose Ω_D values have previously been determined using DTIMS. Then, the drift times are corrected for ion charge states, m/z, etc., and plotted against Ω_D to establish an empirical correlation between the measured drift times with Ω_D.[9-10,77-78] Although the calibration of drift times to Ω_D can be accurate, the results are dependent on the choice of the calibrant ions, and require careful interpretation.[9,36,42,68,71,77] This limitation of TWIMS is less problematic if the technique is to be used solely for ion separation. While the relationship between the drift times from TWIMS and ion Ω_D is not perfectly understood, the Ω_D values measured using TWIMS are quite reproducible,[52-53] and a TWIMS-specific database may be constructed to identify an ion

based on TWIMS Ω_D (though physical context of such Ω_D values may be questionable). Furthermore, efforts are ongoing to understand ion motion in TWIMS,[75-76,79] which are expected to contribute to better interpretation of the experimental results from TWIMS experiments.

TIMS is a recently developed IMS technique with interesting characteristics.[80] In DTIMS and TWIMS, the drift gas is ideally stationary, and a static (DTIMS) or a dynamic electric field (TWIMS) is applied to transport the ions through the drift tube. In TIMS, however, the drift gas flows from the entrance to the exit of a TIMS analyzer to exert a drag force on ions, while an electric field is applied to push the ions against the gas flow (Figure 1c).[18,80-81] If the gas flow and the applied electric field are balanced, no net ion motion across the TIMS analyzer is observed and the ions are trapped inside. If there are ions with different mobilities, ions with lower K, or greater Ω_D, experience greater drag forces by the drift gas. If the electric field is gradually increased axially along the TIMS analyzer, low-mobility ions (greater Ω_D) travel further across the TIMS analyzer until they find a region where the electric field is sufficiently strong to counteract the drag force. With this configuration, trapping of ions can be achieved in a spatially resolved manner. The ions can then be eluted consecutively by gradually decreasing the electric field. Note that, because high-Ω_D ions are trapped downstream of the TIMS analyzer, high-Ω_D ions are eluted first, oppositely form the ion elution order in DTIMS and TWIMS. In addition, TIMS spectra are not plotted with respect to drift time as in DTIMS and TWIMS, but are plotted with respect to elution voltage or ramp time.

The most intriguing aspect of TIMS is that its resolving power can be tuned by adjusting the speed of voltage ramping.[18,81-82] As can be seen in eq 2, without a major change in the instrumentation, small room for resolving power improvement exists in DTIMS, and the situation is similar for TWIMS.[75] Therefore, resolving power tunability is a unique advantage of TIMS that would enable the researchers to operate the instrument optimally in different applications from fast sample screening (fast voltage ramping) to high-resolution mobility separation (slow voltage ramping).

As was the case in TWIMS, calibration of experimental data using known standards is necessary to obtain ion Ω_D. Protocols for Ω_D calibration of TIMS data have previously been described.[81-82]

2.5 High-field asymmetric waveform ion mobility spectrometry (FAIMS) and differential mobility spectrometry (DMS)

The three ion mobility techniques described so far (i.e. DTIMS, TWIMS, and TIMS) are all operated under low-field conditions. Under such conditions, ion motion is relatively well understood and can be correlated to Ω_D. On the contrary, in high fields, ion mobility is no longer constant and becomes dependent on E/N. FAIMS, or DMS (the two terms are sometimes interchangeably[83] or separately[84] used), makes use of this phenomenon for ion separation.

In FAIMS, while ions travel through a drift tube, a high field and a low field are applied alternatively in time in the opposite direction,[83-84] perpendicularly to the drift tube alignment (Figure 1d). The high field is applied for a short period, and the low field is applied for a longer period, so that the products of field strength and applied time for the two conditions are identical. If the mobility of an ion is not dependent on E/N, no net ion motion perpendicular to the drift tube will be observed. In other cases, ions will exhibit perpendicular motion, and ultimately be lost after collision with electrodes that make up the drift tube. Field-dependent ion behaviors are characteristic properties of the ions, so that only a small subset of total ions can travel through the drift tube without being lost. If a compensation field (E_c) is superimposed on to the default electric fields, an ion with a particular perpendicular motion can be chosen and uniquely allowed to travel through the drift tube.

A critical difference between the three low-field IMS techniques introduced and FAIMS is that FAIMS may be considered orthogonal to other analytical tools such as MS. The core parameter determining ion separation in low-field IMS, Ω_D, is highly correlated with ion m/z, and is similar for ions belonging to similar chemical classes. Therefore, the low-field IMS techniques are not completely orthogonal to MS. On the other hand, the variations in the ion mobilities at high fields are highly specific properties of the ions and effective separation may be achieved between ions that cannot be separated by other tools.

A limitation of FAIMS is that only a small portion of the ions are transferred to the exit of the drift tube and other ions are discarded. This makes it necessary to scan the E_c, or the corresponding compensation voltage (CV), if one wishes to examine more than one ion. Inevitably, residence time and ion signal at a CV decrease. In contrast, all ions arrive at the exit of the drift tube and detected in DTIMS, TWIMS, and TIMS. Therefore, FAIMS is more suitable for targeted analysis, similarly to quadrupole-based mass spectrometers.[85]

2.6 Other types of IMS

Novel types of IMS continue to be reported in the literature. The readers are referred to recent reviews for introduction to other types of IMS instruments.[22,86] A recent research paper compares the resolving power of various IMS platforms based on a consistent scale.[87]

3. Ion mobility mass spectrometry (IM-MS)

3.1 Ion mobility time-of-flight mass spectrometry (IM-TOFMS)

Among the variety of mass analyzers that could be coupled with IMS, the time-of-flight (TOF) mass analyzers are predominantly used. This use stems from the fact that

mobility separation in a typical time-dispersive IMS occurs in millisecond time-scale while mass analysis in TOF analyzers occur in microsecond time-scale.[86] In IM-TOFMS configurations, ion packets from the IM section can be sent to the TOF analyzer at regular intervals (a few tens of microseconds, etc.), and full mass analysis of the ions is possible before the following ion packets arrive.[88] The principle of such configuration is similar to liquid chromatography mass spectrometry (LC-MS), in which a faster analysis tool, MS, is placed after LC, minimizing the loss of information from the hyphenation. In fact, IM-MS can also be integrated effectively with LC because the time-scale of IM (milliseconds) fits well between those of LC peak elution (seconds) and TOF mass analysis (microseconds).

An important difference between standalone IMS devices and IM-TOF instruments is the site of ion detection. In typical IM-TOF instruments incorporating time-dispersive IMS techniques such as DTIMS and TWIMS,[86] the 'time ticking' starts when ions are injected into the drift tube, and the time is recorded when the ions arrive at the detector placed at the end of the TOF mass analyzer. In such configuration, measured ion travel time includes not only the time spent inside the drift tube (t_d), but also the time required to travel to and across the TOF analyzer (t_0):

$$t_a = t_d + t_0 \quad (6)$$

The measured ion travel time is referred to as the arrival time (t_a) hereafter. Unlike t_d, t_a is not inversely proportional to the electric field strength E inside the drift tube. Correction for the non-IM component of the arrival times (t_0) is necessary to extract the mobility information of ions. However, accurate characterization of t_0 can be difficult, and this factor is dependent on experimental conditions. In the case of a DTIM-TOF instrument, a convenient resolution exists, based on the fact that t_0 is almost unaffected by the electric field E inside the drift tube, whereas t_d is inversely proportional to E. Therefore, it is possible to find a linear relationship between t_a and E by combining eqs 1 and 6:

$$t_a = \frac{L}{K}\frac{1}{E} + t_0 \quad (7)$$

Equation 7 shows that by performing experiments at multiple electric field strengths, ion mobility K can be inferred from the plot of t_a versus inverse E ($1/E$).[77]

It is possible to combine an IM cell with a mass analyzer other than the TOF, such as the Orbitrap.[89-90] However, such configurations will not be discussed further because currently IM-TOF platforms allow the broadest range of applications.

3.2 Ion fragmentation in IM-MS

Collision-induced dissociation (CID) is frequently utilized in IM-MS platforms for ion fragmentation. It is possible to conduct CID before or after mobility separation of ions. Pre-IM fragmentation (CID-IM-TOFMS) is simple in principle, and can be used to gain mobility information of ion fragments, or to probe structural changes in ions following collisional activation (Figure 4a).[91]

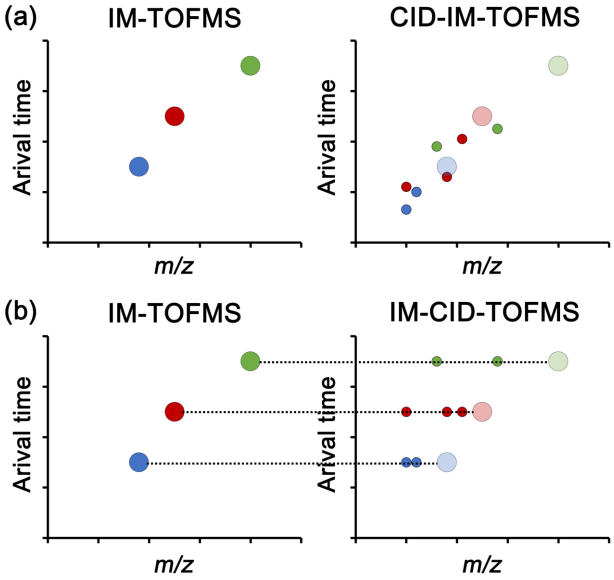

Figure 4. Schematics of ion mobility time-of-flight mass spectrometry (IM-TOFMS) combined with collision-induced dissociation (CID). CID performed in (a) the pre-IM section (CID-IM-TOFMS), and (b) the post-IM section (IM-CID-TOFMS). Large and small data points represent respectively the precursor and fragment ions.

Post-IM ion fragmentation (IM-CID-TOFMS), on the other hand, is an intriguing configuration that is optimal for analytical purposes. When mobility-separated ions are fragmented using CID, arrival times of the fragment ions coincide with those of the precursor ions (Figure 4b),[92-93] because ion fragmentation after IM causes only marginal changes in ion arrival times. In typical liquid chromatography tandem mass spectrometry (LC-MS/MS) experiments, mass selection is necessary before ion fragmentation to relate ion fragments with the precursor ions. This leaves the instrument blind to the unselected, discarded ions. In LC-IM-CID-TOFMS configuration, mass selection is unnecessary because the precursor ion for a fragment ion can be found based on the arrival time, allowing simultaneous fragmentation of all ions. This unique utility of IM has received wide attention, and at the best of the author's knowledge, post-IM fragmentation is implemented in all commercial IM-TOFMS instruments.

As general concepts of IM-MS have been introduced, specific features of three of the most common commercial IM-MS platforms are reviewed in the following sections. No particular commercial platforms are recommended in

this review, as all the instruments have their own advantages and limitations.

3.3 Agilent 6560 drift-tube ion mobility quadrupole time-of-flight mass spectrometer

Details on the Agilent 6560 (Agilent Technologies, Santa Clara, CA) instrument have been described in the literature.[12-13,27,33] This instrument is based on architectures previously developed by Smith and coworkers,[94-96] in which the use of ion funnel[97-98] was critical for ensuring the sensitivity. The instrument is equipped with a ca. 78 cm drift tube.[13,33] As a DTIM instrument, the relationship between experimental data and Ω_D is direct, which is beneficial for standardization of measurements.[33] The default drift gas for the instrument is nitrogen,[13] but a 'Drift Gas Upgrade Kit' can be installed for the use of alternative drift gases such as helium, argon, carbon dioxide, and others.[12] With this upgrade, the default Pirani gauges inside the trapping funnel and the drift cell are replaced with capacitance diaphragm gauges to enable gas-independent pressure measurements, and an electronic pressure controller is also added. Because ions can display different separation characteristics in different drift gases, this option may be advantageous in various applications. In addition, theoretical tools for Ω_D calculations are best developed for ions in helium, and the potential for Ω_D measurement in helium is valuable for fundamental ion structural studies.

It was described above that multiple-*E* experiments are required for accurate determination of ion Ω_D using a DTIM-TOF instrument (eq 7). Such experiments are simple if a sample solution can be infused continuously, but become difficult when the instrument is coupled with LC, owing to the narrow temporal width of a chromatographic peak. To resolve this issue, the instrument supports the 'single-field CCS method,' in which an empirical relationship between arrival times and ion Ω_D values is established using calibrant ions of known Ω_D and utilized in subsequent experiments.[33] Although this method relies on an empirical relationship rather than an accurate relation such as eq 3, ion transport across a DTIM cell is straightforward that unexpectedly large errors from such calibration would not be very common.

Finally, a mass filter and a collision cell are placed between the IM cell and the TOF mass analyzer to allow for post-IM ion selection and fragmentation.

3.4 Waters Synapt quadrupole traveling-wave ion mobility time-of-flight mass spectrometer

Details on the Synapt series instruments (Waters Corp., Wilmslow, UK) have been described in the literature.[14-15,55] In Synapt, a TWIM cell filled with nitrogen drift gas is placed in between two collision cells (the trap and transfer cells). To prevent the loss of ions, ions are confined radially by applying radiofrequency (RF) voltage to the SRIG. A first-generation Syanpt instrument (Synapt G1) was originally equipped with a 18.5 cm TWIM cell, but a current second-generation instrument (Synapt G2) is equipped with a 25.4 cm TWIM cell.[15] In addition, a small (ca. 0.7 cm) cell infused with helium is placed between the trap and the TWIM cells. The helium cell permits an efficient transport of ions at a low pressure region (the trap cell) to a high pressure region (the drift cell).[15] Therefore, higher working pressures can be used to achieve higher resolving power.[15] Concerns on ion heating and fragmentation in the TWIM region exist.[99-100] A study by Williams and coworkers showed that ion heating primarily occurs during injection of ions to the TWIM cell, which can be minimized by increasing the helium cell gas flow rate or decreasing the TWIM cell gas flow rate.[100]

Because of the non-direct relationship between experimentally measured arrival times and ion Ω_D in TWIMS, calibration is required to correlate experimental data with ion Ω_D.[9-10,77-78] The calibration process requires arrival time to be corrected to drift time (eq 6). In DTIM-TOF instruments, the need for accurate determination of t_0 was avoided by utilizing the fact that t_0 of an ion is almost independent on *E* (eq 7). In TWIM-TOF, since the calibration is performed using calibrant ions of distinct Ω_D and *m/z*, t_0 may vary between the ions. Fortunately, ions exiting the TWIM cell are effectively transported to the TOF mass analyzer in a mass-independent manner using traveling waves.[10] Furthermore, the mass-dependent flight times in the TOF mass analyzer can also be estimated and corrected.[10]

Unlike other commercial IM-MS instruments, both pre-IM and post-IM ion fragmentation are possible in Synapt due to the existence of collision cells before (the trap cell) and after (the transfer cell) the IM cell. In addition, due to the long history of the instrument, a wealth of literature exists that describes possible applications and experimental protocols. Note that an alternative TWIM-QqTOF instrument, VIon (Waters Corp. Wilmslow, UK), has also been commercialized.

3.5 Bruker timsTOF trapped ion mobility quadrupole time-of-flight mass spectrometer

Details on timsTOF instruments (Bruker Daltonics, Billerica, MA) have been described in the literature.[17-19] A first-generation timsTOF instrument is equipped with a 46 mm TIMS analyzer, and an entrance and an exit funnel are placed before and after the TIMS analyzer where the ions are focused and transmitted to subsequent regions of the instrument.[18] In the entrance and exit funnels, gaps exist between the electrodes and nitrogen gas flows freely between the plates. However, the electrodes in the TIMS analyzer region are not spaced apart, and the nitrogen gas flows through the TIMS analyzer due to the pressure difference across.[18-19] The small IM cell in timsTOF, is capable of providing surprisingly high resolving power.[81, 101-102] Note that

the resolving power (R_p) of an IMS instrument is typically evaluated similarly to that in mass spectrometers:[87]

$$R_p = \frac{x}{\Delta x} \quad (8)$$

where x is the peak location that can be in units of time (as in eq 1), voltage, and others, depending on the IMS technique utilized, and Δx is the peak width. Although such definition is convenient, it may introduce undesirable bias in some platforms and a careful interpretation is necessary when comparing different platforms. Nevertheless, the TIMS instrument displays an outstanding resolving power also in the Ω_D-based resolving power definition.[87]

Due to the short history of the instrument, relatively small number of TIMS-MS studies have been reported so far. Nonetheless, comprehensive studies are available that characterize the instrumental parameters affecting analytical results,[18-19,80,82,103] including ion heating.[101,104] Recently, a second-generation instrument, timsTOF Pro, has become available, which is equipped with a new TIMS analyzer with an increased length (96 mm).[17] In this design, ions can be accumulated upstream of the TIMS analyzer while ion scanning and elution are performed at the 'analysis region' downstream of the analyzer. Such configuration reduces the need to block ion transmission during the TIMS analysis step, which was necessary for the first-generation instrument,[19] and enhances the instrumental duty cycle. Furthermore, efficient mass selection and fragmentation are possible for ions eluting from the TIMS analyzer.[17, 105] Considering that the TIMS technique uniquely allows resolving power adjustment in the IM section, the improvement in the duty cycle would contribute to a greater popularity of the instrument in IM-MS research.

4. Summary and future outlook

The multidimensional analysis capability offered by IM-MS is showing potential for overcoming current analytical challenges in MS. Construction of Ω_D libraries and development of novel IM-MS architectures are anticipated to further enhance the utility of IM-MS in various applications. In particular, because the core parameter determining separation characteristics in IMS, Ω_D, is not fully orthogonal to *m/z*, enhancement in the resolving power of IM techniques would be valuable. Novel IM techniques with exceptional resolving powers continue to be reported,[106-110] making it possible to expect further advancement in IM-MS.

Acknowledgments

The author acknowledges Prof. Hugh I. Kim at Korea University for his expert guidance on IM-MS research. This publication was supported by the Korea Research Institute of Standards and Science (KRISS) under the project "Establishing Measurement Standards for Inorganic Analysis" (grant no. 17011050) and "Establishment of National Standard System for Nutritional Elements" (grant no. 17011054).

References

1. Paglia, G.; Astarita, G. *Nat. Protoc.* **2017,** 12, 797.
2. Gray, C. J.; Thomas, B.; Upton, R.; Migas, L. G.; Eyers, C. E.; Barran, P. E.; Flitsch, S. L. *BBA-GEN Subjects* **2016,** 1860, 1688.
3. Zheng, X.; Aly, N. A.; Zhou, Y.; Dupuis, K. T.; Bilbao, A.; Paurus, Vanessa L.; Orton, D. J.; Wilson, R.; Payne, S. H.; Smith, R. D.; Baker, E. S. *Chem. Sci.* **2017,** 8, 7724.
4. Hines, K. M.; Ross, D. H.; Davidson, K. L.; Bush, M. F.; Xu, L. *Anal. Chem.* **2017,** 89, 9023.
5. Morsa, D.; Defize, T.; Dehareng, D.; Jérôme, C.; De Pauw, E. *Anal. Chem.* **2014,** 86, 9693.
6. Kim, K.; Lee, J. W.; Chang, T.; Kim, H. I. *J. Am. Soc. Mass Spectrom.* **2014,** 25, 1771.
7. Lapthorn, C.; Pullen, F.; Chowdhry, B. Z. *Mass Spectrom. Rev.* **2013,** 32, 43.
8. Lanucara, F.; Holman, S. W.; Gray, C. J.; Eyers, C. E. *Nat. Chem.* **2014,** 6, 281.
9. Bush, M. F.; Hall, Z.; Giles, K.; Hoyes, J.; Robinson, C. V.; Ruotolo, B. T. *Anal. Chem.* **2010,** 82, 9557.
10. Ruotolo, B. T.; Benesch, J. L. P.; Sandercock, A. M.; Hyung, S. -J.; Robinson, C. V. *Nat. Protoc.* **2008,** 3, 1139.
11. Heck, A. J. R. *Nat. Methods* **2008,** 5, 927.
12. Kurulugama, R. T.; Darland, E.; Kuhlmann, F.; Stafford, G.; Fjeldsted, J. *Analyst* **2015,** 140, 6834.
13. May, J. C.; Goodwin, C. R.; Lareau, N. M.; Leaptrot, K. L.; Morris, C. B.; Kurulugama, R. T.; Mordehai, A.; Klein, C.; Barry, W.; Darland, E.; Overney, G.; Imatani, K.; Stafford, G. C.; Fjeldsted, J. C.; McLean, J. A. *Anal. Chem.* **2014,** 86, 2107.
14. Giles, K.; Pringle, S. D.; Worthington, K. R.; Little, D.; Wildgoose, J. L.; Bateman, R. H. *Rapid Commun. Mass Spectrom.* **2004,** 18, 2401.
15. Giles, K.; Williams, J. P.; Campuzano, I. *Rapid Commun. Mass Spectrom.* **2011,** 25, 1559.
16. Groessl, M.; Graf, S.; Knochenmuss, R. *Analyst* **2015,** 140, 6904.
17. Silveira, J. A.; Ridgeway, M. E.; Laukien, F. H.; Mann, M.; Park, M. A. *Int. J. Mass Spectrom.* **2017,** 413, 168.
18. Michelmann, K.; Silveira, J. A.; Ridgeway, M. E.; Park, M. A. *J. Am. Soc. Mass Spectrom.* **2015,** 26, 14.
19. Silveira, J. A.; Michelmann, K.; Ridgeway, M. E.; Park, M. A. *J. Am. Soc. Mass Spectrom.* **2016,** 27, 585.
20. Cottingham, K. *Anal. Chem.* **2003,** 75, 435 A.
21. Armenta, S.; Alcala, M.; Blanco, M. *Anal. Chim. Acta* **2011,** 703, 114.
22. Cumeras, R.; Figueras, E.; Davis, C. E.; Baumbach, J. I.; Gràcia, I. *Analyst* **2015,** 140, 1376.
23. Mason, E. A.; McDaniel, E. W. *Transport Properties of*

Ions in Gases, Wiley: New York, **1988**.
24. Revercomb, H. E.; Mason, E. A. *Anal. Chem.* **1975,** 47, 970.
25. Kaur-Atwal, G.; O'Connor, G.; Aksenov, A. A.; Bocos-Bintintan, V.; Paul Thomas, C. L.; Creaser, C. S. *Int. J. Ion Mobil. Spectrom.* **2009,** 12, 1.
26. Siems, W. F.; Wu, C.; Tarver, E. E.; Hill, H. H., Jr.; Larsen, P. R.; McMinn, D. G. *Anal. Chem.* **1994,** 66, 4195.
27. May, J. C.; Dodds, J. N.; Kurulugama, R. T.; Stafford, G. C.; Fjeldsted, J. C.; McLean, J. A. *Analyst* **2015,** 140, 6824.
28. Fernandez-Maestre, R. *Int. J. Mass Spectrom.* **2017,** 421, 8.
29. Mason, E. A.; Schamp, H. W. *Ann. Phys.* **1958,** 4, 233.
30. Siems, W. F.; Viehland, L. A.; Hill, H. H. *Anal. Chem.* **2012,** 84, 9782.
31. Wyttenbach, T.; Bleiholder, C.; Bowers, M. T. *Anal. Chem.* **2013,** 85, 2191.
32. Bleiholder, C. *Analyst* **2015,** 140, 6804.
33. Stow, S. M.; Causon, T. J.; Zheng, X.; Kurulugama, R. T.; Mairinger, T.; May, J. C.; Rennie, E. E.; Baker, E. S.; Smith, R. D.; McLean, J. A.; Hann, S.; Fjeldsted, J. C. *Anal. Chem.* **2017,** 89, 9048.
34. May, J. C.; Morris, C. B.; McLean, J. A. *Anal. Chem.* **2017,** 89, 1032.
35. Lalli, P. M.; Corilo, Y. E.; Fasciotti, M.; Riccio, M. F.; de Sa, G. F.; Daroda, R. J.; Souza, G. H. M. F.; McCullagh, M.; Bartberger, M. D.; Eberlin, M. N.; Campuzano, I. D. G. *J. Mass Spectrom.* **2013,** 48, 989.
36. Davidson, K. L.; Bush, M. F. *Anal. Chem.* **2017,** 89, 2017.
37. Dwivedi, P.; Wu, C.; Matz, L. M.; Clowers, B. H.; Siems, W. F.; Hill, H. H. *Anal. Chem.* **2006,** 78, 8200.
38. Ujma, J.; Giles, K.; Morris, M.; Barran, P. E. *Anal. Chem.* **2016,** 88, 9469.
39. Wyttenbach, T.; Helden, G. V.; Batka, J. J.; Carlat, D.; Bowers, M. T. *J. Am. Soc. Mass Spectrom.* **1997,** 8, 275.
40. Mesleh, M. F.; Hunter, J. M.; Shvartsburg, A. A.; Schatz, G. C.; Jarrold, M. F. *J. Phys. Chem.* **1996,** 100, 16082.
41. Young, M. N.; Bleiholder, C. *J. Am. Soc. Mass Spectrom.* **2017,** 28, 619.
42. Bleiholder, C.; Johnson, N. R.; Contreras, S.; Wyttenbach, T.; Bowers, M. T. *Anal. Chem.* **2015,** 87, 7196.
43. Kim, H. I.; Johnson, P. V.; Beegle, L. W.; Beauchamp, J. L.; Kanik, I. *J. Phys. Chem. A* **2005,** 109, 7888.
44. Eiceman, G. A.; Nazarov, E. G.; Stone, J. A. *Anal. Chim. Acta* **2003,** 493, 185.
45. Laszlo, K. J.; Bush, M. F., *J. Phys. Chem. A* **2017**, 121, 7768.
46. Shvartsburg, A. A.; Schatz, G. C.; Jarrold, M. F. *J. Chem. Phys.* **1998,** 108, 2416.
47. von Helden, G.; Hsu, M. T.; Gotts, N.; Bowers, M. T. *J. Phys. Chem.* **1993,** 97, 8182.
48. Boschmans, J.; Jacobs, S.; Williams, J. P.; Palmer, M.; Richardson, K.; Giles, K.; Lapthorn, C.; Herrebout, W. A.; Lemiere, F.; Sobott, F. *Analyst* **2016,** 141, 4044.
49. Seo, J.; Warnke, S.; Gewinner, S.; Schollkopf, W.; Bowers, M. T.; Pagel, K.; von Helden, G. *Phys. Chem. Chem. Phys.* **2016,** 18, 25474.
50. Siems, W. F.; Viehland, L. A.; Hill, H. H. *Analyst* **2016,** 141, 6396.
51. Fernandez-Maestre, R.; Harden, C. S.; Ewing, R. G.; Crawford, C. L.; Hill, H. H. *Analyst* **2010,** 135, 1433.
52. Paglia, G.; Angel, P.; Williams, J. P.; Richardson, K.; Olivos, H. J.; Thompson, J. W.; Menikarachchi, L.; Lai, S.; Walsh, C.; Moseley, A.; Plumb, R. S.; Grant, D. F.; Palsson, B. O.; Langridge, J.; Geromanos, S.; Astarita, G. *Anal. Chem.* **2015,** 87, 1137.
53. Paglia, G.; Williams, J. P.; Menikarachchi, L.; Thompson, J. W.; Tyldesley-Worster, R.; Halldórsson, S.; Rolfsson, O.; Moseley, A.; Grant, D.; Langridge, J.; Palsson, B. O.; Astarita, G. *Anal. Chem.* **2014,** 86, 3985.
54. Marchand, A.; Livet, S.; Rosu, F.; Gabelica, V. *Anal. Chem.* **2017,** 89, 12674.
55. Pringle, S. D.; Giles, K.; Wildgoose, J. L.; Williams, J. P.; Slade, S. E.; Thalassinos, K.; Bateman, R. H.; Bowers, M. T.; Scrivens, J. H. *Int. J. Mass Spectrom.* **2007,** 261, 1.
56. Kirk, A. T.; Raddatz, C. -R.; Zimmermann, S. *Anal. Chem.* **2017,** 89, 1509.
57. Shvartsburg, A. A.; Clemmer, D. E.; Smith, R. D. *Anal. Chem.* **2010,** 82, 8047.
58. D'Atri, V.; Porrini, M.; Rosu, F.; Gabelica, V. *J. Mass Spectrom.* **2015,** 50, 711.
59. Lee, J. W.; Kim, H. I. *Analyst* **2015,** 140, 661.
60. Shvartsburg, A. A.; Jarrold, M. F. *Chem. Phys. Lett.* **1996,** 261, 86.
61. Alexeev, Y.; Fedorov, D. G.; Shvartsburg, A. A. *J. Phys. Chem. A* **2014,** 118, 6763.
62. Shvartsburg, A. A.; Liu, B.; Jarrold, M. F.; Ho, K. -M. *J. Chem. Phys.* **2000,** 112, 4517.
63. Anderson, S. E.; Bleiholder, C.; Brocker, E. R.; Stang, P. J.; Bowers, M. T. *Int. J. Mass Spectrom.* **2012,** 330-332, 78.
64. Bleiholder, C.; Contreras, S.; Bowers, M. T. *Int. J. Mass Spectrom.* **2013,** 354-355, 275.
65. Bleiholder, C.; Contreras, S.; Do, T. D.; Bowers, M. T. *Int. J. Mass Spectrom.* **2013,** 345-347, 89.
66. Bleiholder, C.; Wyttenbach, T.; Bowers, M. T. *Int. J. Mass Spectrom.* **2011,** 308, 1.
67. Kim, H.; Kim, H. I.; Johnson, P. V.; Beegle, L. W.; Beauchamp, J. L.; Goddard, W. A.; Kanik, I. *Anal. Chem.* **2008,** 80, 1928.
68. Kim, H. I.; Kim, H.; Pang, E. S.; Ryu, E. K.; Beegle, L. W.; Loo, J. A.; Goddard, W. A.; Kanik, I. *Anal. Chem.* **2009,** 81, 8289.
69. Campuzano, I.; Bush, M. F.; Robinson, C. V.; Beaumont, C.; Richardson, K.; Kim, H.; Kim, H. I. *Anal. Chem.* **2012,** 84, 1026.
70. Siu, C. -K.; Guo, Y.; Saminathan, I. S.; Hopkinson, A. C.; Siu, K. W. M. *J. Phys. Chem. B* **2010,** 114, 1204.
71. Lee, J. W.; Davidson, K. L.; Bush, M. F.; Kim, H. I.

Analyst **2017,** 142, 4289.
72. Lapthorn, C.; Pullen, F. S.; Chowdhry, B. Z.; Wright, P.; Perkins, G. L.; Heredia, Y. *Analyst* **2015,** 140, 6814.
73. Lee, J. W.; Lee, H. H. L.; Davidson, K. L.; Bush, M. F.; Kim, H. I. *manuscript in preparation*.
74. Thalassinos, K.; Slade, S. E.; Jennings, K. R.; Scrivens, J. H.; Giles, K.; Wildgoose, J.; Hoyes, J.; Bateman, R. H.; Bowers, M. T. *Int. J. Mass Spectrom.* **2004,** 236, 55.
75. Shvartsburg, A. A.; Smith, R. D. *Anal. Chem.* **2008,** 80, 9689.
76. Giles, K.; Wildgoose, J. L.; Langridge, D. J.; Campuzano, I. *Int. J. Mass Spectrom.* **2010,** 298, 10.
77. Bush, M. F.; Campuzano, I. D. G.; Robinson, C. V. *Anal. Chem.* **2012,** 84, 7124.
78. Thalassinos, K.; Grabenauer, M.; Slade, S. E.; Hilton, G. R.; Bowers, M. T.; Scrivens, J. H. *Anal. Chem.* **2009,** 81, 248.
79. Mortensen, D. N.; Susa, A. C.; Williams, E. R. *J. Am. Soc. Mass Spectrom.* **2017,** 28, 1282.
80. Fernandez-Lima, F.; Kaplan, D. A.; Suetering, J.; Park, M. A. *Int. J. Ion Mobil. Spectrom.* **2011,** 14, 93.
81. Silveira, J. A.; Ridgeway, M. E.; Park, M. A. *Anal. Chem.* **2014,** 86, 5624.
82. Hernandez, D. R.; DeBord, J. D.; Ridgeway, M. E.; Kaplan, D. A.; Park, M. A.; Fernandez-Lima, F. *Analyst* **2014,** 139, 1913.
83. Swearingen, K. E.; Moritz, R. L. *Expert Rev. Proteomics* **2012,** 9, 505.
84. Schneider, B. B.; Nazarov, E. G.; Londry, F.; Vouros, P.; Covey, T. R. *Mass Spectrom. Rev.* **2016,** 35, 687.
85. Sinatra, F. L.; Wu, T.; Manolakos, S.; Wang, J.; Evans-Nguyen, T. G. *Anal. Chem.* **2015,** 87, 1685.
86. May, J. C.; McLean, J. A. *Anal. Chem.* **2015,** 87, 1422.
87. Dodds, J. N.; May, J. C.; McLean, J. A. *Anal. Chem.* **2017,** 89, 12176.
88. Hoaglund, C. S.; Valentine, S. J.; Sporleder, C. R.; Reilly, J. P.; Clemmer, D. E. *Anal. Chem.* **1998,** 70, 2236.
89. Ibrahim, Y. M.; Garimella, S. V. B.; Prost, S. A.; Wojcik, R.; Norheim, R. V.; Baker, E. S.; Rusyn, I.; Smith, R. D. *Anal. Chem.* **2016,** 88, 12152.
90. Keelor, J. D.; Zambrzycki, S.; Li, A.; Clowers, B. H.; Fernandez, F. M. *Anal. Chem.* **2017,** 89, 11301.
91. Lee, J. W.; Park, M. H.; Ju, J. T.; Choi, Y. S.; Hwang, S. M.; Jung, D. J.; Kim, H. I. *Mass Spectrom. Lett.* **2016,** 7, 16.
92. Hoaglund-Hyzer, C. S.; Lee, Y. J.; Counterman, A. E.; Clemmer, D. E. *Anal. Chem.* **2002,** 74, 992.
93. Fernandez-Lima, F. A.; Becker, C.; Gillig, K. J.; Russell, W. K.; Tichy, S. E.; Russell, D. H. *Anal. Chem.* **2009,** 81, 618.
94. Tang, K.; Shvartsburg, A. A.; Lee, H. -N.; Prior, D. C.; Buschbach, M. A.; Li, F.; Tolmachev, A. V.; Anderson, G. A.; Smith, R. D. *Anal. Chem.* **2005,** 77, 3330.
95. Ibrahim, Y. M.; Baker, E. S.; Danielson, W. F.; Norheim, R. V.; Prior, D. C.; Anderson, G. A.; Belov, M. E.; Smith, R. D. *Int. J. Mass Spectrom.* **2015,** 377, 655.
96. Baker, E. S.; Clowers, B. H.; Li, F.; Tang, K.; Tolmachev, A. V.; Prior, D. C.; Belov, M. E.; Smith, R. D. *J. Am. Soc. Mass Spectrom.* **2007,** 18, 1176.
97. Kelly, R. T.; Tolmachev, A. V.; Page, J. S.; Tang, K.; Smith, R. D. *Mass Spectrom. Rev.* **2010,** 29, 294.
98. Ibrahim, Y.; Tang, K.; Tolmachev, A. V.; Shvartsburg, A. A.; Smith, R. D. *J. Am. Soc. Mass Spectrom.* **2006,** 17, 1299.
99. Morsa, D.; Gabelica, V.; De Pauw, E. *Anal. Chem.* **2011,** 83, 5775.
100. Merenbloom, S. I.; Flick, T. G.; Williams, E. R. *J. Am. Soc. Mass Spectrom.* **2012,** 23, 553.
101. Ridgeway, M. E.; Silveira, J. A.; Meier, J. E.; Park, M. A. *Analyst* **2015,** 140, 6964.
102. Jeanne, K.; Fouque, D.; Garabedian, A.; Porter, J.; Baird, M.; Pang, X.; Williams, T. D.; Li, L.; Shvartsburg, A.; Fernandez-lima, F. *Anal. Chem.* **2017,** 89, 11787.
103. Fernandez-Lima, F. A.; Kaplan, D. A.; Park, M. A. *Rev. Sci. Instrum.* **2011,** 82, 126106.
104. Liu, F. C.; Kirk, S. R.; Bleiholder, C. *Analyst* **2016,** 141, 3722.
105. Meier, F.; Beck, S.; Grassl, N.; Lubeck, M.; Park, M. A.; Raether, O.; Mann, M. *J. Proteome Res.* **2015,** 14, 5378.
106. Glaskin, R. S.; Ewing, M. A.; Clemmer, D. E. *Anal. Chem.* **2013,** 85, 7003.
107. Merenbloom, S. I.; Glaskin, R. S.; Henson, Z. B.; Clemmer, D. E. *Anal. Chem.* **2009,** 81, 1482.
108. Deng, L.; Ibrahim, Y. M.; Hamid, A. M.; Garimella, S. V. B.; Webb, I. K.; Zheng, X.; Prost, S. A.; Sandoval, J. A.; Norheim, R. V.; Anderson, G. A.; Tolmachev, A. V.; Baker, E. S.; Smith, R. D. *Anal. Chem.* **2016,** 88, 8957.
109. Deng, L.; Webb, I. K.; Garimella, S. V. B.; Hamid, A. M.; Zheng, X.; Norheim, R. V.; Prost, S. A.; Anderson, G. A.; Sandoval, J. A.; Baker, E. S.; Ibrahim, Y. M.; Smith, R. D. *Anal. Chem.* **2017,** 89, 4628.
110. Giles, K.; Ujma, J.; Wildgoose, J. L.; Green, M. R.; Richardson, K.; Langridge, D. J.; Tomczyk, N. 65th Annual American Society for Mass Spectrometry Conference, Indianapolis, IN, June 4-8, 2017, www.waters.com/posters (accessed November 2017).